Journal on Oncology

www.journalononcology.org

Research Article

Open Access, Volume 3

The Value of MRI-Based Radiomic Nomograms in Differential Diagnosis and Metastasis Prediction of Rhabdomyosarcoma and Neuroblastoma in Children

Jiheng Wu[1]; Xuan Jia[2]; Xinyi Shou[3]; Wenqi Wang[2]; Lei Liu[4]; Jinhu Wang[5]; Hongfei Ni[6]; Hongxi Zhang[2]*; Shaoqing Ni[1,7]*

[1]National Clinical Trial Institute, Children's Hospital, Zhejiang University School of Medicine, National Clinical Research Center for Child health, Hangzhou, China.

[2]Department of Radiology, Children's Hospital Affiliated to Zhejiang University School of Medicine, Hangzhou, China.

[3]Children's Hospital, Zhejiang University School of Medicine, National Clinical Research Center for Child Health, Hangzhou, China.

[4]Department of Pathology, Children's Hospital, Zhejiang University School of Medicine, National Clinical Research Center for Child Health, Hangzhou, China.

[5]Department of Surgical Oncology, Children's Hospital, Zhejiang University School of Medicine, National Clinical Research Center for Child Health, Hangzhou, Chin

[6]Innovation Institute for Artificial Intelligence in Medicine of Zhejiang University, College of Pharmaceutical Sciences, Zhejiang University, Hangzhou, China.

[7]Research Center for Clinical Pharmacy, Zhejiang University, Hangzhou, China.

Abstract

Background: Rhabdomyosarcoma (RMS) and Neuroblastoma (NB) are highly malignant soft tissue sarcoma with tendency to metastasize. Due to the similarities in clinical manifestations and imaging features between RMS and NB, they are often misdiagnosed, which resulted in improper treatment progression of the mass. On the other hand, the treatment paradigm for patients with metastasis RMS/NB and non-metastasis RMS/NB is different. Preoperative abdominal Magnetic Resonance Imaging (MRI) can provide valuable information for differential diagnosis and metastasis prediction to support surgical decisions. This study aimed to develop MRI-based whole-volume tumor radiomic signatures for differential diagnosis and metastasis prediction.

Methods: We retrospectively sampled 40 patients (21 patients with RMS and 19 patients with NB). Using Least Absolute Shrinkage and Selection Operator (LASSO) regression and stepwise logistic regression, a classification model and a metastasis prediction model based on MRI radiomic signatures were constructed. Nomograms were established by integrating the MRI information for better classification and prediction. Harrell's concordance index (C-index) and time-dependent Receiver Operating Characteristic (ROC) curves were used as performance evaluating metrics.

Manuscript Information: *Received: Jul 03, 2023; Accepted: Aug 02, 2023; Published: Aug 09, 2023*

Correspondance: *Hongxi Zhang & Shaoqing Ni, Children's Hospital Zhejiang University School of Medicine, 3333 Binsheng Rd, Hangzhou, Zhejiang, P.R. China, 310052.*

Email: chgcp@zju.edu.cn & hongxizhang11@zju.edu.cn

Citation: *Wu J, Jia X, Shou X, Zhang H, Ni S, et al. The Value of MRI-Based Radiomic Nomograms in Differential Diagnosis and Metastasis Prediction of Rhabdomyosarcoma and Neuroblastoma in Children. J Oncology. 2023; 3(2): 1099.*

Results: The nomograms consisting of radiomic signatures demonstrated good discrimination and calibration in classification (Area Under the Curve [AUC] =89.97%) and metastasis prediction (AUC=82.25%). The calibration curve and GiViTI calibration belt value analysis indicated that the radiomic nomograms can be used in clinical practice.

Conclusions: MRI-based whole-tumor radiomic signatures have excellent performance for differential diagnosis and metastasis prediction in pediatric RMS and NB. Radiomic nomograms may aid in preoperative risk assessment and guide personalized treatment strategies for pediatric soft tissue sarcomas.

Keywords: Rhabdomyosarcoma; Neuroblastoma; Radiomics; MRI; Differential diagnosis; Metastasis prediction.

Introduction

Rhabdomyosarcoma (RMS) and Neuroblastoma (NB) are the most prevalent malignant soft-tissue tumor in children [1,2]. The most common primary site for these tumors is the abdomen. Differential diagnosis and metastatic diagnosis of these pediatric sarcomas is essential to selecting an appropriate treatment [3]. Differential diagnosis of sarcomas such as RMS and NB is usually made by imaging tests and histological examination after surgical resection or puncture biopsy, which can lead to delay in treatment. This method, however may be time-consuming and cause excessive damage to the patient. Besides, this method of differential diagnosis can be very demanding based on the experience level of the attending pathologist/radiologist. Due to the similarities in imaging features and clinical manifestations, RMS and NB are often misdiagnosed [4]. Outcome in patients with localized RMS/NB is generally good, but outcome for patients with metastatic RMS/NB remains poor with 3-year Overall Survival (OS) of 34%-56% [5,6]. Therefore, a non-invasive and effective tool to distinguish RMS from NB and predict the probability of metastasis is very important for diagnosis and treatment.

A recently developed method of data processing and image analysis, radiomics, is able to obtain features that cannot be directly identified by direct human visualization on medical images and can discover new information about tumor grades, genetics, curative effect, and prognosis [7,8]. Radiomic parameters can be applied in clinical decision support systems to improve the accuracy of diagnostic, predictive, and prognostic. Recently, the radiomic characteristics of Magnetic Resonance Imaging (MRI) have been shown to have potential for histological subtype classification [9]. Dong et al. proposed a radiomic nomogram can predict the number of lymph node metastasis in locally advanced gastric cancer [10]. However, to the best of our knowledge, it is unclear whether radiomics analysis based on MR imaging can be use in differential diagnosis and metastasis prediction of RMS and NB.

Immunostaining of Ki-67 is used as a biomarker for tumor proliferation. It has been shown that Ki-67 expression strongly correlates with prognosis and clinical behavior of soft tissue sarcomas [11,12]. Nevertheless, its strength as a prognostic factor in RMS and NB is still unclear.

Our hospital has conducted plain and enhanced MRI for the diagnosis of RMS and NB. Therefore, the aim of this study was to assess the application of Ki-67 and MRI radiomics based on the sequence: T2_SPIR_AX-MVXD_HR_RT for differential diagnosis and metastasis prediction of RMS and NB (Figure 1). This study provides information for early accurate diagnosis, which has important clinical application value.

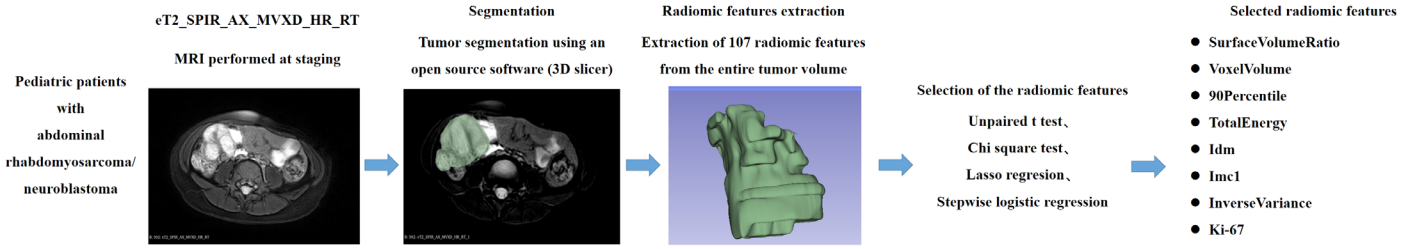

Figure 1: Workflow of MRI radiomic nomogram modeling for differential diagnosis and metastasis prediction.

Patients and methods

Patients

The institutional review board approved this retrospective study, and the need to obtain informed consent was waived. Patients who underwent MRI from Feburary 2015 to June 2022 in were retrospectively analyzed. The inclusion criteria were as follows: (1) Patients with histopathological examination and with complete clinicopathological information; (2) Primary tumor MRI was performed before chemotherapy and surgery. The exclusion criteria were as follows: (1) poor quality or incomplete MR images.

Imaging data acquisition and processing

All MR images were obtained on a 3T Philips Achieva MRI scanner (Philips Healthcare, The Netherlands). Regions Of Interest (ROI) were manually segmented by an experienced radiologist using 3D-Slicer software, version 4.9.1 (www.slicer.org) and reviewed by another MRI physicist. The open-source package PyRadiomics within 3D Slicer was used to extract the radiomic features.

Statistical analysis

R software (version 3.4.0) was used to perform all statistical analyses in this study. All radiomic features were normalized with

z-score so that get a standard normal distribution of image intensities. Student's t-test was used to compare differences between the two groups of continuous variables. The chi-squared test was used to compare the differences between the two groups of categorical variables. Least Absolute Shrinkage and Selection Operator (LASSO) regression was performed to select the initial factors and prevent overfitting of multifactorial models. Logistic regression analysis was used to evaluate the prognostic value of the selected radiomic features for the corresponding outcome. The level of significance for all statistical analyses was set at $p<0.05$.

Results

Of the 40 patients included in this study, 19 were affected by NB and 21 were affected by RMS. 20 patients had metastatic spread (12 in the NB cohort and 8 in the RMS cohort). With selection by LASSO regression analysis, eight radiomic features and Ki-67 were determined to potentially have significant roles in distinguishing NB from RMS (Supplementary Material Figure S1).

Using an unpaired t test and a chi-square test, two radiomic parameters (90 Percentile; Imc1) and Ki-67 showed statistically significant differences between NB and RMS. Compared with RMS, NB was associated with a lower value of 90 Percentile (p=0.0020), higher value of Imc1 (p=0.0233) and values of Ki-67 (p=0.0366) (Table 1).

Table 1: Comparison of selected radiomic features and proliferation marker according to histotype.

Mean±SD	Neuroblastoma (NB)	Rhabdomyosarcoma (RMS)	*p* value
Mesh Volume	108156.37 ± 111039.23	165801.82 ± 254430.34	0.353 [a]
Surface Volume Ratio	0.24 ± 0.10	0.31 ± 0.22	0.174 [a]
Voxel Volume	108352.46 ± 111206.66	166031.39 ± 254650.66	0.354 [a]
90 Percentile	1226.10 ± 359.75	1580.33 ± 314.22	**0.002** [a]
Total Energy	116800685626 ± 194213887210	260925719851 ± 386132366622	0.141 [a]
Idm	0.27 ± 0.10	0.29 ± 0.13	0.700 [a]
Imc1	-0.17 ± 0.04	-0.24 ± 0.13	**0.023** [a]
Inverse Variance	0.25 ± 0.06	0.21 ± 0.06	0.051 [a]
Ki-67	0.17 ± 0.25	0.37 ± 0.32	**0.037** [a]
Metastasis (%)	12 (63.16)	8 (38.10)	0.206 [b]

[a]Unpaired t test; b Yates' continuity corrected chi-square test.

Using stepwise logistic regression analysis, with AIC=41.12, four of the nine features, Voxel Volume, 90 Percentile, Idmn, Imc1, were correlated with differential diagnosis between RMS and NB (Table 2). The final features are shown in supplementary A1. The 90 Percentile feature was found to be significantly higher in RMS (1580.33 ± 314.22 vs. 1226.10 ± 359.75, p= 0.00895). The logistic regression model showed an 89.97% accuracy in classifying RMS and NB. The C-index was 0.9 (95% CI: 0.808-0.992).

Table 2: Risk factors for differential diagnosis between RMS and NB.

Coefficients:	OR (95% CI)	Pr(>|z|)
VoxelVolume	11.20490 (1.641, 181.841)	0.083 .
90 Percentile	27.69881 (4.440, 314.726)	**0.009 ****
Idmn	0.00145 (0.000000959, 0.235)	0.097 .
Imc1	0.05853 (0.001, 0.408)	0.071 .

The GiViTI calibration belt values were used to evaluate the precision and discrimination of the model, which are shown in Figure 2. The 80% CI (light gray area) and 95% CI (dark gray area) in the calibration belt plot crossed the diagonal bisector line. The P-value in the GiViTI calibration test was 0.971, suggesting that the model was well calibrated.

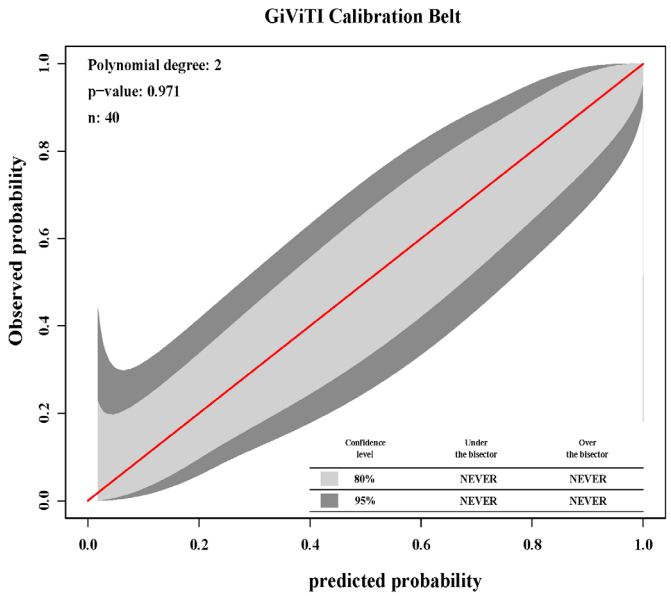

Figure 2: Calibration of the nomogram for differential diagnosis between NB and RMS. The 80% CI and 95% CI of GiViTI calibration belt did not surpass the diagonal line.

For differential diagnosis between the metastasis and non-metastasis cohorts, LASSO logistic regression analysis allowed for the selection of three potential features: Surface Volume Ratio; Imc1; Inverse Variance (Supplementary Material Figure S2, Table 3). Stepwise logistic regression analysis, with AIC=45.08 showed that two of the three features, Imc1 and Inverse Variance were correlated with differential diagnosis between metastasis and non- metastasis cohorts (Table 4). The final features are shown in supplementary A1. Inverse Variance was found to be significantly higher in the metastatic cohort (0.017 ± 0.431 *vs.* -0.396 ± 0.370, p=0.002). The logistic regression model showed an accuracy of 82.25% in classifying RMS and NB.

Table 3: Comparison of selected radiomic features and proliferation markers between the metastatic cohort and non-metastatic cohorts.

Mean±SD	Metastatic	Non-metastatic	*p* value
Surface Volume Ratio	-0.698±0.211	-0.389±0.511	**0.017** [a]
Imc1	0.744±0.184	0.458±0.567	**0.039** [a]
InverseVariance	0.017±0.431	-0.396±0.370	**0.002** [a]
Ki-67	0.234±0.306	0.370±0.369	0.212 [a]

[a] Unpaired t test.

Table 4: Risk factors for metastasis prediction.

Coefficients:	OR (95% CI)	Pr(>|z|)
Imc1	0.387 (1.143, 1.902)	0.017 *
InverseVariance	0.534 (1.335, 2.197)	**0.001 ****

The GiViTI calibration belt values were used to evaluate the precision and discrimination of the model, which are shown in Figure 3. The 80% CI (light gray area) and 95% CI (dark gray area) in the calibration belt plot crossed the diagonal bisector line. The P-value in the GiViTI calibration test was 0.828, suggesting that the model was well calibrated.

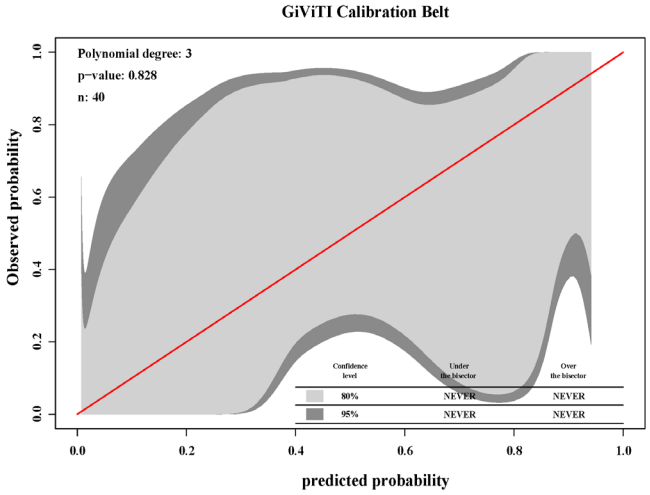

Figure 3: Calibration of the nomogram for metastasis prediction. The 80% CI and 95% CI of the GiViTI calibration belt did not surpass the diagonal line.

Based on multivariate logistic analyses, a differential diagnosis model was established using Voxel Volume, 90 Percentile, Idmn, and Imc1. The metastasis prediction model was constructed using Imc1 and Inverse Variance. The nomograms converted from the combination models are shown in Figures 4 and 5. The model based on nomogram discrimination showed excellent performance. ROC composition plots and calibration curves were used as performance metrics of the nomograms, and the application of the nomogram showed outstanding advantages over the relevant threshold ranges (Figures 6 and 7).

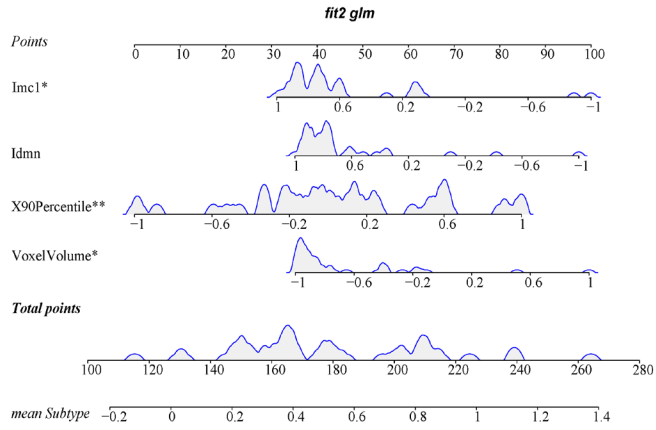

Figure 4: Nomogram based on the radiomic signature for differential diagnosis.

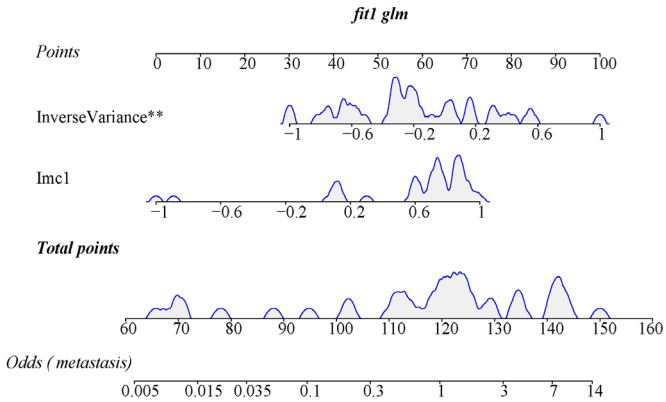

Figure 5: Nomogram based on the radiomic signature for metastasis prediction.

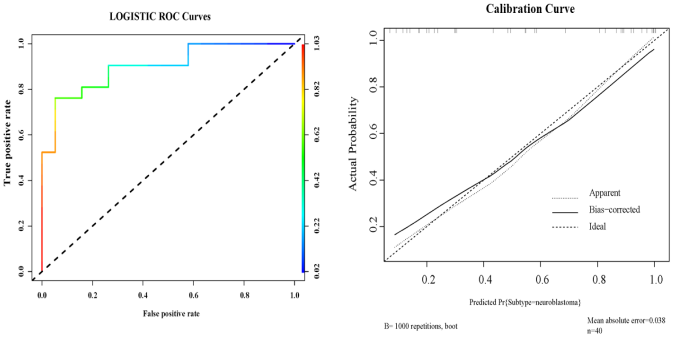

Figure 6: ROC curve and calibration curve of nomogram for differential diagnosis.

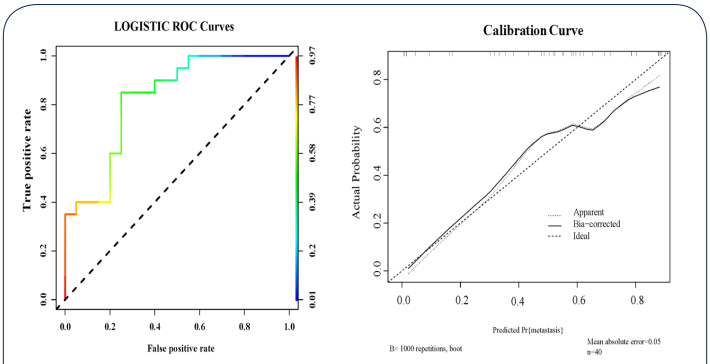

Figure 7: ROC curve and calibration curve of nomogram for metastasis prediction.

Discussion

In this study, we demonstrated that incorporating Axial T2 (spectral presaturation inversion recovery, SPIR) MRI into a radiomic model improved the diagnostic performance for distinguishing between RMS and NB, and for metastasis prediction, with excellent discriminative power and calibration. Furthermore, this study provides a non-invasive and effective prediction tool to distinguish between RMS and NB and predict probability of metastasis. By applying significant radiomic parameters, we developed validated nomograms for noninvasive, individualized differential diagnosis and metastasis prediction. This finding could be useful in several contexts, such as in helping physicians better understand the risk of disease progression, and in aiding them to make better treatment recommendations.

RMS and NB are heterogeneous at both the genetic and histopathological levels [13]. The chemotherapy regimens for RMS and NB differ significantly. The chemotherapy regimen for RMS may include VA (vincristine and dactinomycin) or VAC (vincristine, dactinomycin, and cyclophosphamide), which is very different from the chemotherapy regimen for NB (carboplatin, etoposide et al.) [14,15]. However, risk stratification and treatment plans according to metastasis also differ [16-19]. For patients with metastatic RMS/NB, lymph node dissection could be an effective way to reduce the risk of recurrence and improve prognosis. Therefore, accurate differential diagnoses and metastasis prediction are beneficial for treatment determination and risk stratification for patients with sarcoma [20]. Non-invasive differential diagnosis between RMS and NB has been a challenge in pediatric sarcoma [21]. Currently, differential diagnosis of RMS and NB relies on Ultrasound (US) and MRI for preliminary identification [22,23]. Furthermore, NB biomarkers (neuron enolase, etc.) and biopsies are used to make definite diagnoses, which inevitably causes injury in pediatric patients [24,25]. Currently, there is no mature technology for non-invasive differential diagnosis and metastasis prediction for these tumor types.

Radiomics can noninvasively capture histology related intratumoral and intertumoral heterogeneity in voxels, identify phenotypes, and provides additional metastatic information [26].

A previous study pointed out that MRI features were associated with pathological subtype, angiogenesis and peritumoral infiltration [27]. Recently, the development of algorithms and medical image analysis has promoted differential diagnosis and precision medicine in pediatric sarcomas [28,29]. Radiomic signatures may provide more sensitive and accurate information regarding tumor type, malignancy and metastasis [30,31]. Our study demonstrated that Voxel Volume, 90 Percentile, Idmn, and Imc1 represent four potential radiomic features closely associated with MRI differences between RMS and NB, and that Imc and Inverse Variance represented two potential radiomic features closely associated with probability of metastasis. As an independent risk factor, a higher value of 90 Percentile probably indicates RMS as opposed to NB, and a higher value of Inverse Variance probably indicates metastases. These two parameters can be used as classification indicator to distinguish RMS from NB, and to indicate metastases in RMS/NB.

Prior to this study, few efforts using radiomic application had been made for rare disease. This is the first study to apply radiomics for the differential diagnosis, and metastasis prediction of RMS and NB. As differential diagnoses between RMS and NB requires special training and the expertise of a radiologist, our findings may provide support for such expertise. This study does, however, haves some limitations. Most notably, because of their rarity, the generalization ability and robustness of the model need further study.

There are several directions for future extension of this study. First is to expand our classification and metastasis prediction models to RMS and NB subtypes using different algorithm and to include more available MR images for training. Secondly, integrating different dimensions of patient data, such as genomic data and prognostic data, into our framework is our key goal. By combining genetic information with image feature information, a better prognostic model may be established for risk prediction in pediatric sarcoma patients.

Conclusions

The MRI-based radiomic model developed in this study has a higher clinical value for the noninvasive diagnosis of RMS and NB, and for metastasis prediction. However, before applying this method in a real-world setting, more studies are needed to validate the performance of radiomic nomograms.

Declarations

Consent to publish: Not applicable.

Availability of data and materials: The datasets used and/or analyzed during the current study available from the corresponding author on reasonable request.

Competing interests: The authors declare that they have no competing interests.

Funding: This research was funded by Open Foundation of Key Laboratory of Digital Technology in Medical Diagnostics of Zhejiang Province (Grant No. SZZD202217), National Natural Science Foundation of China (Grant No. 81573516).

Acknowledgement: We sincerely appreciate all the patients who participated in this study.

Authors Contribution: JH W conceived the idea, reviewed, and edited the manuscript. JH W, XJ, LL, and HF N carried out research selection, data extraction, and statistical analysis. WQ W, JHW and XY S contributed to literature retrieval. All authors contributed to

this article and approved the submitted version.

References

1. Shern JF, et al. Genomic Classification and Clinical Outcome in Rhabdomyosarcoma: A Report from an International Consortium. J Clin Oncol. 2021; 39: 2859-2871.
2. Chava, S, et al. miR-15a-5p, miR-15b-5p, and miR-16-5p inhibit tumor progression by directly targeting MYCN in neuroblastoma. Mol Oncol. 2020; 14: 180-196.
3. Sangkhathat, S, Current management of pediatric soft tissue sarcomas. World J Clin Pediatr. 2015; 4: 94-105.
4. Taieb D, et al. European Association of Nuclear Medicine Practice Guideline/Society of Nuclear Medicine and Molecular Imaging Procedure Standard 2019 for radionuclide imaging of phaeochromocytoma and paraganglioma. Eur J Nucl Med Mol Imaging. 2019; 46: 2112-2137.
5. Toledo RA, et al. Consensus Statement on next-generation-sequencing-based diagnostic testing of hereditary phaeochromocytomas and paragangliomas. Nat Rev Endocrinol. 2017; 13: 233-247.
6. van Berkel AK. Pacak JW. Lenders, Should every patient diagnosed with a phaeochromocytoma have a (1)(2)(3) I-MIBG scintigraphy? Clin Endocrinol (Oxf). 2014; 81: 329-33.
7. Lambin, P, et al. Radiomics: the bridge between medical imaging and personalized medicine. Nat Rev Clin Oncol, 2017. 14(12): p. 749-762.
8. Spadarella G, et al. MRI based radiomics in nasopharyngeal cancer: Systematic review and perspectives using Radiomic Quality Score (RQS) assessment. Eur J Radiol. 2021; 140: 109744.
9. Majzner RG, et al. CAR T Cells Targeting B7-H3, a Pan-Cancer Antigen, Demonstrate Potent Preclinical Ac-tivity Against Pediatric Solid Tumors and Brain Tumors. Clin Cancer Res. 2019; 25: 2560-2574.
10. Dong D, et al. Deep learning radiomic nomogram can predict the number of lymph node metastasis in lo-cally advanced gastric cancer: an international multicenter study. Ann Oncol. 2020; 31: 912-920.
11. Choong PF, Akerman M, Willén H, et al. Prognostic value of Ki-67 expression in 182 soft tissue sarcomas. Proliferation--a marker of metastasis?. APMIS. 1994; 102: 915-924.
12. Hoos A, Stojadinovic A, Mastorides S, et al. High Ki-67 proliferative index predicts disease specific survival in patients with high-risk soft tissue sarcomas. Cancer. 2001; 92: 869-874.
13. Berbegall AP, et al. Heterogeneous MYCN amplification in neuroblastoma: A SIOP Europe Neuroblastoma Study. Br J Cancer. 2018; 118: 1502-1512.
14. Croteau N, J Nuchtern, MP LaQuaglia, Management of Neuroblastoma in Pediatric Patients. Surg Oncol Clin N Am. 2021; 30: 291-304.
15. Rogers TN, R Dasgupta. Management of Rhabdomyosarcoma in Pediatric Patients. Surg Oncol Clin N Am. 2021; 30: 339-353.
16. Haduong JH, et al. An update on rhabdomyosarcoma risk stratification and the rationale for current and future Children's Oncology Group clinical trials. Pediatr Blood Cancer. 2022; 69: e29511.
17. Tolbert VP, KK Matthay. Neuroblastoma: Clinical and biological approach to risk stratification and treat-ment. Cell Tissue Res. 2018; 372: 195-209.
18. Swift CC, et al. Updates in Diagnosis, Management, and Treatment of Neuroblastoma. Radiographics, 2018. 38: 566-580.
19. Rhee DS, et al. Update on pediatric rhabdomyosarcoma: A report from the APSA Cancer Committee. J Pe-diatr Surg. 2020; 55: 1987-1995.
20. Eary JF, EU Conrad. Imaging in sarcoma. J Nucl Med. 2011; 52: 1903-13.
21. Inarejos CE, et al. MRI of Rhabdomyosarcoma and Other Soft-Tissue Sarcomas in Children. Radiographics. 2020; 40: 791-814.
22. Gurria JP, R Dasgupta. Rhabdomyosarcoma and Extraosseous Ewing Sarcoma. Children (Basel). 2018; 5.
23. Freling, N.J, et al. Imaging findings in craniofacial childhood rhabdomyosarcoma. Pediatr Radiol. 2010; 40: 1723-38.
24. Odelstad, L, et al. Neuron specific enolase: a marker for differential diagnosis of neuroblastoma and Wilms' tumor. J Pediatr Surg. 1982; 17: 381-5.
25. Devin CL, et al. The morbidity of open tumor biopsy for intraabdominal neoplasms in pediatric patients. Pediatr Surg Int. 2021; 37: 1349-1354.
26. Gill AB, et al. Correlating Radiomic Features of Heterogeneity on CT with Circulating Tumor DNA in Meta-static Melanoma. Cancers (Basel). 2020. 12.
27. Lo, G.R, et al. Combining molecular and imaging metrics in cancer: Radiogenomics. Insights Imaging. 2020. 11: 1.
28. van Timmeren JE, et al. Radiomics in medical imaging-"how-to" guide and critical reflection. Insights Imag-ing, 2020; 11: 91.
29. Madhogarhia, R, et al. Radiomics and radiogenomics in pediatric neuro-oncology: A review. Neurooncol Adv. 2022; 4: vdac083.
30. Luo X, et al. Radiomic Signatures for Predicting Receptor Status in Breast Cancer Brain Metastases. Front Oncol. 2022; 12: 878388.
31. Zhu C, et al. Prediction of distant metastasis in esophageal cancer using a radiomics-clinical model. Eur J Med Res. 2022; 27: 272.